Vacuum 87 (2013) 89–94

Contents lists available at SciVerse ScienceDirect

Vacuum

journal homepage: www.elsevier.com/locate/vacuum

Sliding wear resistance of tempered D6ac steel

Shyh-Chi Wu [a,b], Hua-Chiang Wene [a,e], Kuang-Hung Tseng [c], Wei-Hung Yau [d,*], Ming-Jhang Wu [a], Chang-Pin Chou [a], Wen-Kuang Hsu [e]

[a] Department of Mechanical Engineering, National Chiao Tung University, Hsinchu 300, Taiwan, ROC
[b] Chung Shan Institute of Science and Technology (CSIST), Taoyuan 325, Taiwan, ROC
[c] Institute of Materials Engineering, National Pingtung University of Science and Technology, Pingtung 91201, Taiwan, ROC
[d] Department of Mechanical Engineering, Chin-Yi University of Technology, Taichung 411, Taiwan, ROC
[e] Department of Materials Science and Engineering, National Tsing Hua University, Hsinchu 300, Taiwan, ROC

ARTICLE INFO

Article history:
Received 27 February 2012
Received in revised form
4 June 2012
Accepted 4 June 2012

Keywords:
Temper
Friction
Elongation
Tribology

ABSTRACT

The aim of this study was to determine the sliding wear resistance of D6ac (tempered at room temperature, 450, or 550 °C) and to perform tribological responds. The obtained microstructures exhibited a heavy number of misfit dislocations from work hardening of the parent material, with the degree of disorder dislocation decreasing gradually upon increasing the temperature from 450 to 550 °C. XRD spectra observed that the residual austenite and/or mixed structures of ferrite with the precipitation of carbides at 550 °C will result in a softer state than that of the room temperature specimen. The elevated temperature affected the tribological behavior and induced in the parent material a significant surface response failure. The lateral force increased gradually up to 50 μN in the tempered cases, due to the enhanced toughness. We suggest that the increase in the coefficients of friction upon increasing the tempering temperature from 450 to 550 °C resulted due to a soft ferrite phase. Slightly stable fluctuations of the values of μ appeared for the surfaces scratched at a constant load; therefore, plastic deformation occurred along the wear path. For the measured results of the D6ac from room temperature to 550 °C, the coefficient of friction was 0.34 ± 0.05, 0.27 ± 0.04, and 0.13 ± 0.02, respectively. The experimental result also can be evidenced from tribological stressing and mechanical behavior.

1. Introduction

The percentage reduction of D6ac (medium-carbon low-alloy steel) can be controlled using the flow-forming method as well as electron beam welding, but the specimens still require annealing treatment [1–5]. The mechanical properties of D6ac change considerably upon decreasing the impact of annealing treatment after performing weld thermal cycles [5,6]. The main technical problem is the increased brittleness of the parent material [7]. Notably, extensive prior cold work can dramatically decrease the steel's toughness; the weld metal can also influence the tensile properties [8,9]. Indeed, the tribological behavior is an important limiting factor affecting the quality of the parent metal. The increased wear resistance of the metal has become a major concern to researchers. Tribological behavior is, therefore, assessed in terms of sliding wear characteristics [10]. Scratch technology can be applied for direct processing of the material's surface using a nano-sized tip. The friction coefficient and volume loss are usually evaluated under lubricated and non-lubricated conditions at different sliding speeds as well as at different sliding distances [11,12]. Under tribological contact, the brittleness of the parent material is increased as a result of the increased thermal treatment temperature; the increased friction coefficient is usually a result of a different microstructure. This analytical approach has several advantages, including the free selection of materials, simple design alteration, and convenient initial facilities [13–17]. To separate the influence of the brittleness of the parent material from that of thermal tempering, in this study we performed tribological and wear experiments using flow-forming D6ac.

2. Experimental details

D6ac is a low-alloy vacuum-melted steel containing several other elements and featuring a carbon content of 0.42–0.48%. D6ac was designed primarily for use at room temperature, with a tensile strength in the range 1800–2000 MPa and good ductility (ASM

* Corresponding author. No.57, Sec. 2, Zhongshan Rd., Taiping Dist., Taichung 41170, Taiwan, R.O.C. Tel.: +886 4 23924505; fax: +886 4 23930062.
E-mail addresses: wsg0314@emallfly.com.tw (S.-C. Wu), a091316104@gmail.com, a091316104@yahoo.com.tw (H.-C. Wene), jon73120647@gmail.com (M.-J. Wu), cpchou@mail.nctu.edu.tw (C.-P. Chou), wkhsu@mx.nthu.edu.tw (W.-K. Hsu).

0042-207X/$ – see front matter © 2012 Elsevier Ltd. All rights reserved.
http://dx.doi.org/10.1016/j.vacuum.2012.06.005

1981) [18]. Table 1 revealed that the chemical compositional analysis: the contents of all elements were within the ranges expected for standard D6ac (AMS 6431). The chemical composition of steel was determined using energy dispersive X-ray spectrometry (EDS) and a carbon determination technique. D6ac steel plates were treated using the following procedure: (i) the D6AC steel was obtained using vacuum arc remelting (AMS 6431). (ii) Prior to performing the flow-forming process, the D6AC steel was subjected to normalizing treatment (910 ± 14 °C), with a holding time of 105 min and subsequent cooling in air. (iii) Flow-forming of the D6AC steel was performed in a three-roller spinning machine (roller angles: 15, 20, and 30°) with the percentage reduction controlled at 67%; details of the spinning machine conditions have been reported previously by Jahazi and Ebrahimi [2]. Each specimen had a thickness of 9.9 mm; the feed rate was 0.7 mm rpm^{-1}. (iv) Solution treatment was performed with all of the specimens under the same conditions (900 °C/30 min/air cooling). (v) To relieve stress, the specimens were subjected to tempering treatment at 450 and 550 °C (T-450 and T-550) for 2 h, followed by cooling in air.

Tensile test specimens were prepared following the guidelines of ASTM standard E370. These specimens were separated by laser cutting along the axis direction of the tube, following ASTM standard E8a (ASM 1997) [19]. The strain rate applied was 0.2 mm min^{-1}, prior to the yield strength being reached. The tribological properties of the specimens were determined through scratch tests performed using atomic force microscopy (AFM, Digital Instruments Nanoscope III) in conjunction with a nano-indentation measurement system (Hysitron); a constant scan speed of 2 μm s^{-1} was applied. To determine the coefficients of friction of D6ac steel initiated at low-constant-force modes of sliding cycles, the specimens were subjected to constant loads of 500 μN. In addition, for surface investigation of sliding wear, the rough tip (radius: 2 mm) was applied to the specimens at room temperature; the corresponding surface profiles were examined in the constant forces mode. Scanning electron microscopy (SEM, Hitachi S-4300, Tokyo, Japan) was used to characterize the morphology of the specimens from EDS analysis. Microstructural characterization of the specimens under sliding wear was performed using optical microscopy (OM). The microstructures of the specimens were also observed using a transmission electron microscope (TEM, JEOL, JEM-2100F) operated at 200 kV. Crystallinity of the specimens were analyzed by X-ray diffraction (PANalytical X'Pert Pro (MRD)), with Cu Kα ($\lambda = 0.154$ nm) radiation for 2θ from 35° to 75° at a scan speed of 2° min^{-1}, and a grazing angle of 0.5° under 30 kV and 30 mA.

3. Results and discussion

3.1. Microstructure and element analysis

Fig. 1a displays a TEM image of the original D6ac steel at room temperature. We observed a heavy degree of misfit dislocations as a result of work hardening. Dislocation multiplication or dislocation nucleation appeared to induce some extended grain shapes during the forming process. The degree of disorder dislocation decreased after the specimen had been tempered at 450 °C [Fig. 1b]. We also observed a few dislocation multiplications when the specimen was tempered at 550 °C [Fig. 1c]. These results match those reported by Jahazi et al. [5], who noted that the microstructure of the fully annealed material consisted of spherodized cementite distributed uniformly in the ferrite matrix and grain boundaries. We suspect that large nucleation of dislocation occurred during the cold deformation process in the initial stage [Fig. 1a]; the fine cementite particles elongated during the spinning process [5]. Fig. 1d shows XRD spectra obtained from the room temperature and the samples temped at 550 °C. The performing of D6ac steel has been observed to cause transformation of the material into body centered cubic martensite at room temperature. The relative peak intensities of the room temperature samples and 550 °C samples corresponded to the position at 44.58° (011) and 64.98° (002). The maximum intensity at room temperature was observed in the (011) peak position. The peak intensities of the α-phase in the 550 °C samples are the same as the room temperature samples. However, residual austenite (weak peak at 44°) was formed after tempering at 550 °C. It is important to avoid immediate fracture impact from heavy cold working by means of additional tempering treatment. The gradual change in the microstructure of D6ac indicates that tempering treatment helped to eliminate dislocations as well as residual stress. Fig. 2 presents the fractography set of the tempered specimens [(a) room temperature, (b) 450 °C, (c) 550 °C]; the EDS analysis reveals the percentage of atoms as well as the weight. The content (atomic %) of carbon atoms decreased from 39.40 to 0 % and that of ferrite elements increased from 29.75 to 73.82% upon increasing the tempering temperature from room temperature to 550 °C. We suggest that the microstructure comprised cementite distributed uniformly with grain boundaries [5] [Fig. 2a]. The cementite phase transformed, however, into a ferrite matrix with grain boundaries after tempering at up to 550 °C, with decreasing levels of carbon atoms occurring at the same time [Fig. 2b and c].

3.2. Mechanical properties

At suitable temperatures, medium-carbon low-alloy steel usually consists of ferrite, austenite, cementite, and martensite. In a previous study [20], the fracture characteristics of D6ac, with relatively coarse and discrete carbides at prior austenite grain boundaries, were evidenced after tempering at high temperatures. Our experimental data suggest that the microstructure [Fig. 1] has a strong affect on the yield strength (YS), ultimate tensile strength (UTS), and elongation in Table 2. We found that the YS and UTS were greater after tempering at 450 to 550 °C than they were at room temperature. During tempering (aging), the micro-constituents presumably dissolved into the soft ferrite. We also expected residual stress to be present in the parent material. Jahazi et al. [5] observed a substantial increase in the tensile strength (YS increased from 508.2 to 660.7 MPa; UTS increased from 632.7 to 762.3 MPa) of the material after quenching and tempering, relative to that of the cold deformed material (YS = 228.7 MPa; UTS = 388.3 MPa). We found evidence that tempering without quenching could directly enhance YS and UTS after cold deforming. The tempering process provides energy to the parent material,

Table 1
Chemical composition of D6ac steel (wt %).

Element	C	Mn	P	S	Si	Cr	Ni	Mo	V	Fe
Specification AMS 6431	0.42–0.48	0.6–0.9	0.01	0.01	0.15-0.3	0.9–1.2	0.4–0.7	0.9–1.1	0.08–0.15	Bal.
Used in this work (average concentration values)	0.47	0.8	0.01	0.01	0.27	0.98	0.55	1.05	0.1	Bal.

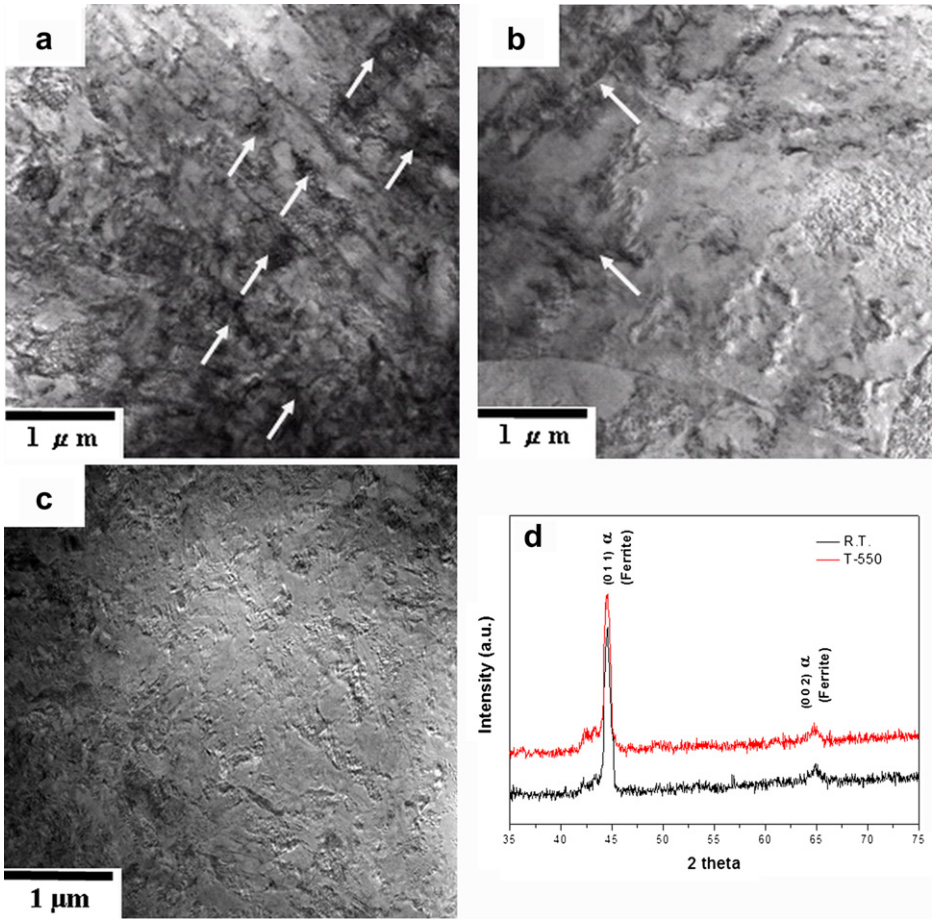

Fig. 1. TEM images of the microstructures of the D6ac samples at (a) room temperature and (b, c) after tempering at (b) 450 and (c) 550 °C. The mark with arrows is the dislocation multiplication or dislocation nucleation zone.

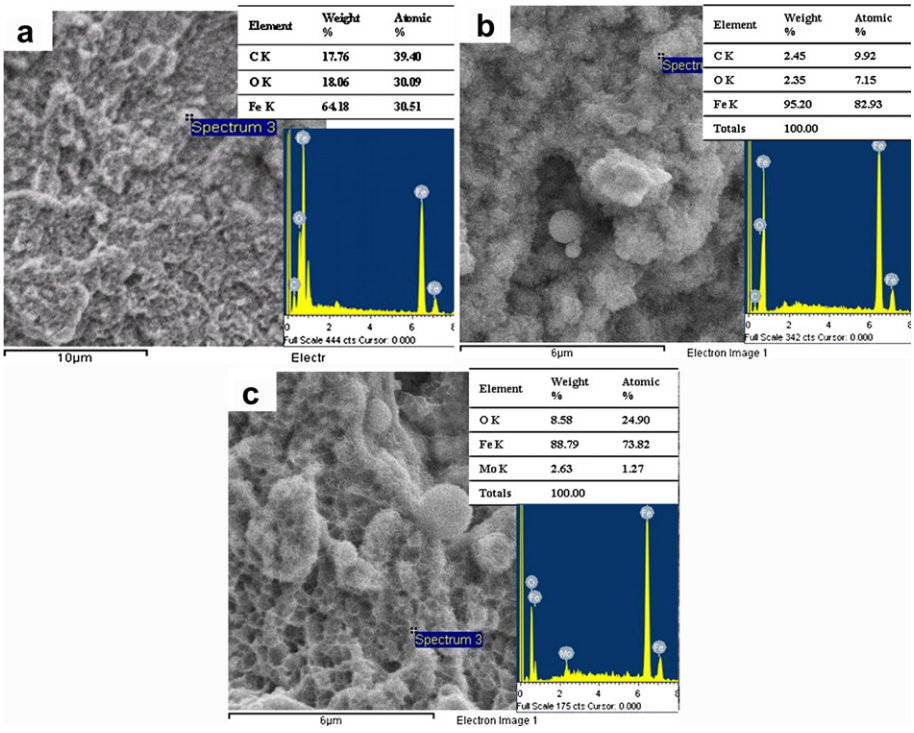

Fig. 2. SEM images and EDS profiles of the D6ac samples at (a) room temperature and (b, c) after tempering at (b) 450 and (c) 550 °C.

Table 2
Mechanical properties and friction coefficients of flow-formed D6ac steel materials subjected to tempering heat treatment.

Sample code	Heat treating process	YS (0.2% offset), MPa	UTS, MPa	Elongation (gauge 50.8 mm), %	Friction coefficient: plate zone
D6AC-RT	Solution	608.3	608.3	0.5	0.34 ± 0.05
D6AC-450	Solution + tempering	1096	1278	10.1	0.27 ± 0.04
D6AC-550	Solution + tempering	832	958	11.6	0.13 ± 0.02

potentially increasing the toughness of the cold working parts, particular for flow-forming D6ac at the onset of elongation. Wei et al. [13] examined the relationship between the hardness and impact toughness of H13 steel after tempering. They suggested that specimens tempered under suitable conditions could provide higher wear resistance in adhesive wear. We were encouraged, therefore, to study the stability of the flow-forming D6ac under sliding conditions.

3.3. Tribological behavior

To compare the tribological behavior of the D6ac, we examined the effect of the tempering temperature on the sliding wear of the parent material. Abrasion of all of the specimens was initiated at a constant force during the sliding cycles. Fig. 3 presents images of the sliding wear of the samples at (a) room temperature and after tempering at (b) 450 and (c) 550 °C; they provide strong evidence for a non-uniform grain boundary in the parent material that correspond area is mark with arrows. The observable damage resulted from the asperity tips on the contacting metal, with shearing and rupturing of the adhesive surface as a result of local contact pressure during sliding. We readily observe corresponding wear debris from the presented sliding traces [Fig. 3a], a typical characteristic of adhesive wear. In addition, some crack lines appeared as a result of brittleness, which caused some delaminated craters and wear debris as well. It appears that as the tempering temperature increased, the proportion of small oxide patches increased slightly, along with small amount of wear debris and

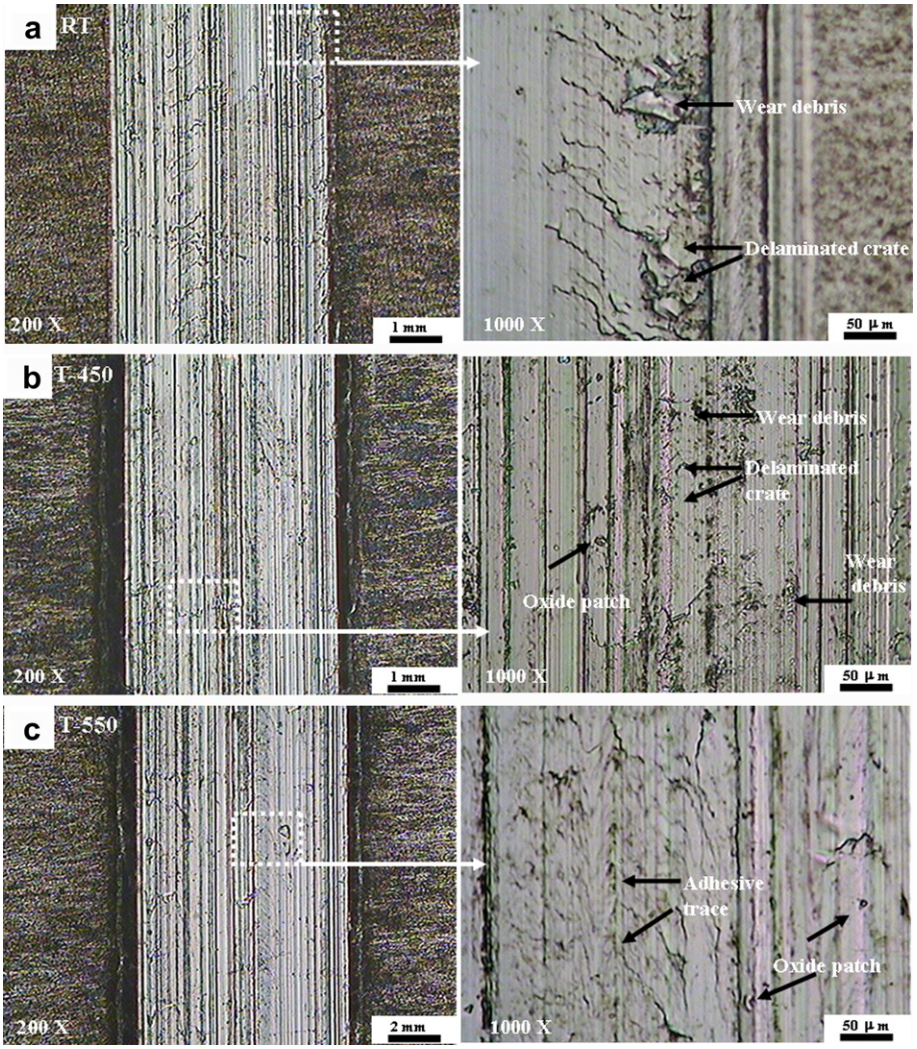

Fig. 3. OM images of the sliding wear of the D6ac samples at (a) room temperature and (b, c) after tempering at (b) 450 and (c) 550 °C. The magnification of the samples are both 200× (left picture) and 1000× (right picture).

delaminated craters [Fig. 3b]. Fracture damage increased dramatically, with curved cracks aligned roughly perpendicular to the direction of scratching, after tempering at 550 °C. One can compare the sliding surface and the ductility damage that produces delaminated craters on the worn surface with a relatively smooth surface and regular outline [Fig. 3c]. Wei et al. [13] reported that the wear rate depended on the tempering temperature; that is to say, the wear debris with a relatively smooth surface and regular outline would be expected. Fig. 4a plots the fluctuations in lateral force with respect to the duration. The lateral force increased gradually up to 50 μN, due to the increased toughness, after increasing the

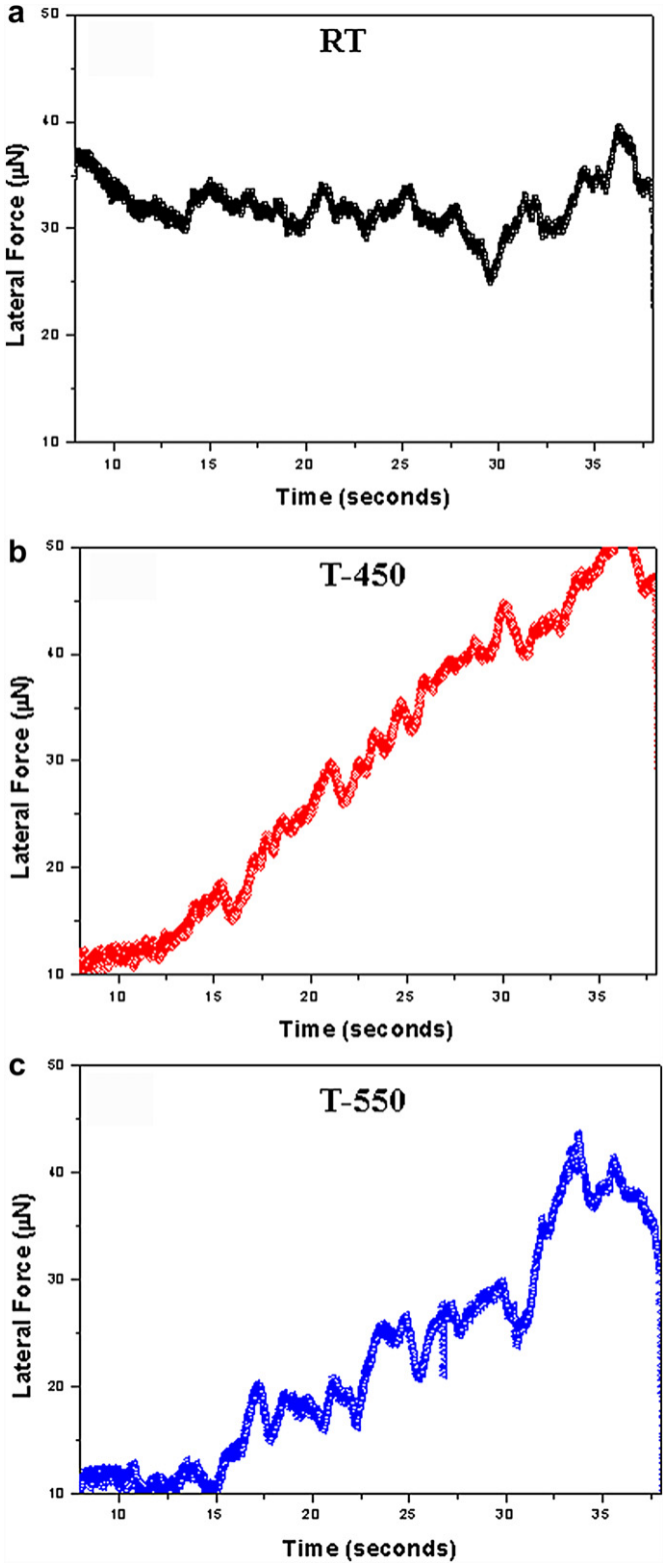

Fig. 4. Fluctuations in lateral force plotted with respect to the duration of displacement of the D6ac samples at (a) room temperature and (b, c) after tempering at (b) 450 and (c) 550 °C.

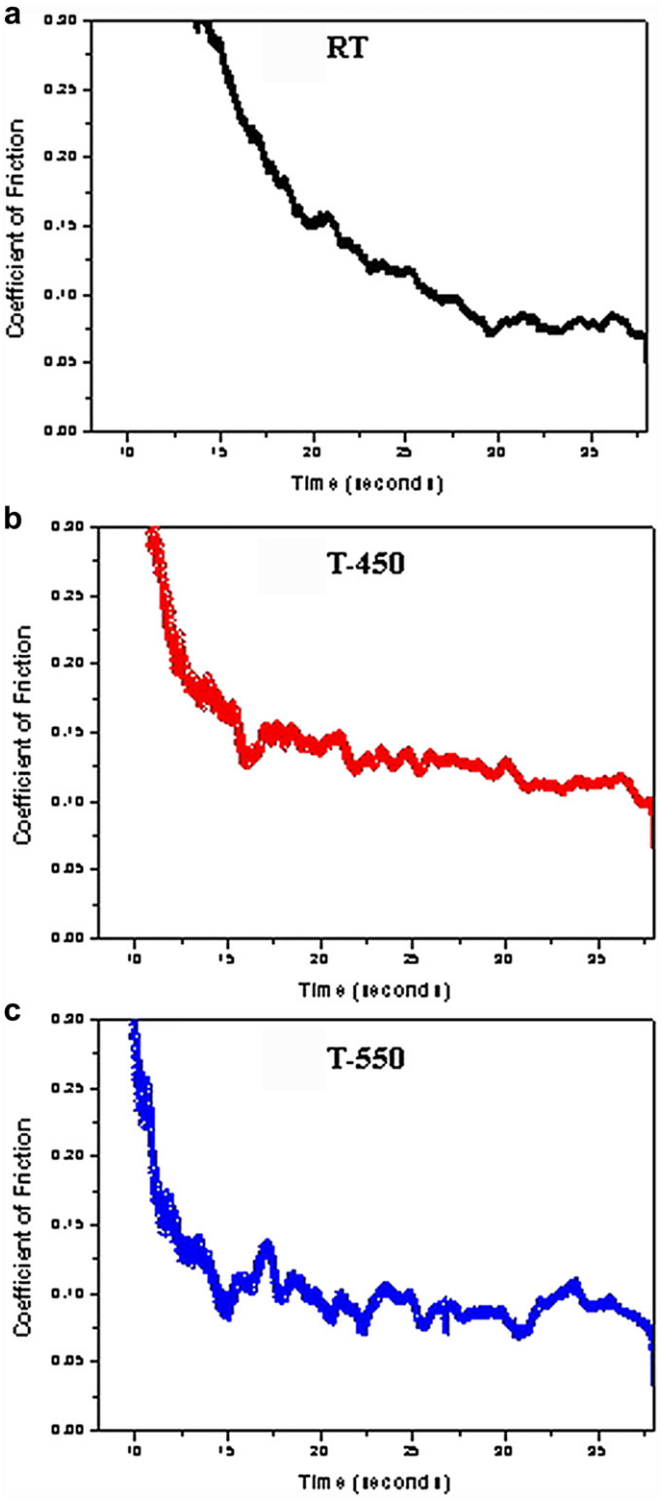

Fig. 5. The fluctuations of the values of μ of the D6ac samples at (a) room temperature and (b, c) after tempering at (b) 450 and (c) 550 °C.

tempering temperature from 450 to 550 °C [Fig. 4b and c]. Eventually, the scratch surface suffered from brittleness to ductility damage of the parent material; the morphology could be determined from the observed fluctuations in lateral force. Recently, the tribological stressing, abrasive wear behavior, and wear transitions of steel samples have been reported to depend upon their friction coefficients, volume losses, lubricated and non-lubricated conditions, different sliding speeds, and different temperatures [13–16]. The effects of HSS [21], alloy [22–27], and iron [28] have been determined from tribological and wear investigations.

Fig. 5a also shows the fluctuations of the values of μ of the room temperature specimens. Again, adhesion and delamination were revealed by the indenter as the tip moved backward. Adhesion and delamination became the predominant wear mechanisms behind the decreases in the values of μ because increasing the tempering temperature. Slightly stable fluctuations of the values of μ appeared for the surfaces scratched at a constant load; therefore, plastic deformation occurred along the wear path [Fig. 5b and c]. These results were expected due to the higher temperature decreased the number of contact asperities.

The degrees of adhesion (Fig. 3) and the sliding effect (Figs. 4 and 5) have been well reported. Therefore, we suggest that tempering treatment can increase elongation as a result of the soft ferrite phase when tempering at high temperatures. For the D6ac samples tempered at room temperature, 450 °C, and 550 °C, we measured coefficients of friction of 0.34 ± 0.05, 0.27 ± 0.04, and 0.13 ± 0.02, respectively. When taken into consideration with the data in Table 2, these results support the trend in the effect of tempering and provide a reasonable estimate of the magnitude of the scratching damage of the parent material. We suspect that the D6ac material was affected by the diffusion of the input fusion heat, such that part of the parent metal experienced recovery and stress relief. The microstructures were dependent on the tempering treatment variables [8,9]. We systematically determined that the trend in the dislocation density transfer was the reason for the changes in the values of YS, UTS, and elongation. We have taken care to present the sliding damage introduced to the D6ac material in terms of an examination of the lateral forces and the friction coefficients.

4. Conclusion

We have employed a combination of scratch techniques to investigate the contact-induced deformation of D6ac steel that had been subjected to tempering. Controlling the tool roughness in the sliding test was a critical step. XRD spectra observed that the preforming of D6ac steel has been observed to cause transformation of the material into body centered cubic martensite at room temperature; however, residual austenite was formed after tempering at 550 °C. TEM analysis of the parent material revealed a heavy degree of misfit dislocations from work hardening; the degree of disorder dislocations decreased gradually upon elevating the tempering temperature. We have compared the morphological changes with respect to the lateral forces and friction coefficients. The scratch resistance decreased upon increasing the lateral force of the parent material. The scratch resistance was affected by the weak adhesion of the parent material; ductility track lines appeared after tempering at elevated temperatures. The tested properties varied somewhat in terms of sensitivity with respect to those of the parent material. The YS, UTS, and elongation were greater after tempering at 450 and 550 °C than they were at room temperature.

Acknowledgment

This study was supported by the National Science Council of the Republic of China (NSC-99-2221-E-009-031-MY2) and by the National Nano Device Laboratories in Taiwan (NDL99-C03S-042). The author would like to thank Prof. W.K. Hus, Dr. H.C. Wen (Department of Materials Science and Engineering, National Tsing Hua University, Hsinchu 300, Taiwan, ROC): kindly to support the services of equipment (Transmission electron microscopy).

References

[1] Lakshminarayanan AK, Balasubramanian V. Materials and Manufacturing Processes 2011;26:868.
[2] Yao ZK, Wang T, Guo HZ, Yang X. Science and Technology of Welding and Joining 2011;27:1701.
[3] Han WT, Wan FR, Leng B, Ukai S, Tang QX, Hayashi S, et al. Science and Technology of Welding and Joining 2010;16:690.
[4] Balasubramanian TS, Balakrishnan M, Balasubramanian V, Muthu Manickam MA. Science and Technology of Welding and Joining 2010;16:702.
[5] Jahazi M, Ebrahimi G. Journals of Materials Processing Technology 2000;103:362.
[6] Notvest K. Welding Journal 1966;45:173S.
[7] Cheng CM, Chou CP, Lee IK, Kuo IC. Journals of Materials Science and Technology 2006;22:685.
[8] Song M, Guan K. Engineering Failure Analysis 2011;18:1613.
[9] Tavares SSM, Pardal JM, Corte JS, Scandian C, Herculano LFG. Engineering Failure Analysis 2009;16:1765.
[10] Azevedo CRF, Marques ER. Engineering Failure Analysis 2010;17:286.
[11] Tuckart W, Gregorio M, Iurman L. Surface Engineering 2010;26:185.
[12] Sergejev F, Peetsalu P, Sivitski A, Saarna M, Adoberg E. Engineering Failure Analysis 2011;18:1689.
[13] Wei MX, Wang SQ, Wang L, Cui XH, Chen KM. Tribology International 2011;44:898.
[14] Hubner W. Tribology International 2001;34:231.
[15] Modi AP. Tribology International 2007;40:490.
[16] Hiratsuka K, Inagaki M. Tribology International 2012;49:39.
[17] Beake BD, Bell GA, Goodes SR, Pickford NJ, Smith JF. Surface Engineering 2010;26:37.
[18] ASM magnesium alloysMetals handbook. 9th ed., vol. 4. ASM; 1981. p. 122.
[19] ASM International. Metals handbook, vol. 6. Ohio: Materials Park; 1997. 254.
[20] Chang TL, Tsay LW, Chen C. Materials Science and Engineering A 2001;316:153.
[21] Leskovšeka V, Kalinb M, Vižintin J. Vacuum 2006;80:507.
[22] Hejwowski T. Vacuum 2006;80:1326.
[23] Cai F, Zhou C, Wang N, Gong S, Xu H. Vacuum 2006;81:85.
[24] Campagna V, Bowers R, Northwood DO, Sun XC, Bauerle P. Surface Engineering 2011;27:86.
[25] Lei MK, Zhou Q, Ou YX, Song TK, Guo Y. Surface Engineering 2010;26:277.
[26] O'Donnell LJ, Michal GM, Ernst F, Kahn H, Heuer AH. Surface Engineering 2010;26:284.
[27] Korkut MH, Gok MS. Surface Engineering 2009;25:517.
[28] Tarkowski P, Budzynski P, Kasietczuk W. Vacuum 2005;78:679.